# Обзор ArXiv: astro-ph, Март 1-3, 2017

От Сильченко О.К.

# Astro-ph: 1703.00449

THE FORMATION OF THE FIRST QUASARS IN THE UNIVERSE

JOSEPH SMIDT[1], DANIEL J. WHALEN[2], JARRETT L. JOHNSON[1] AND HUI LI[1]

*Draft version March 3, 2017*

# Куб с холодными потоками

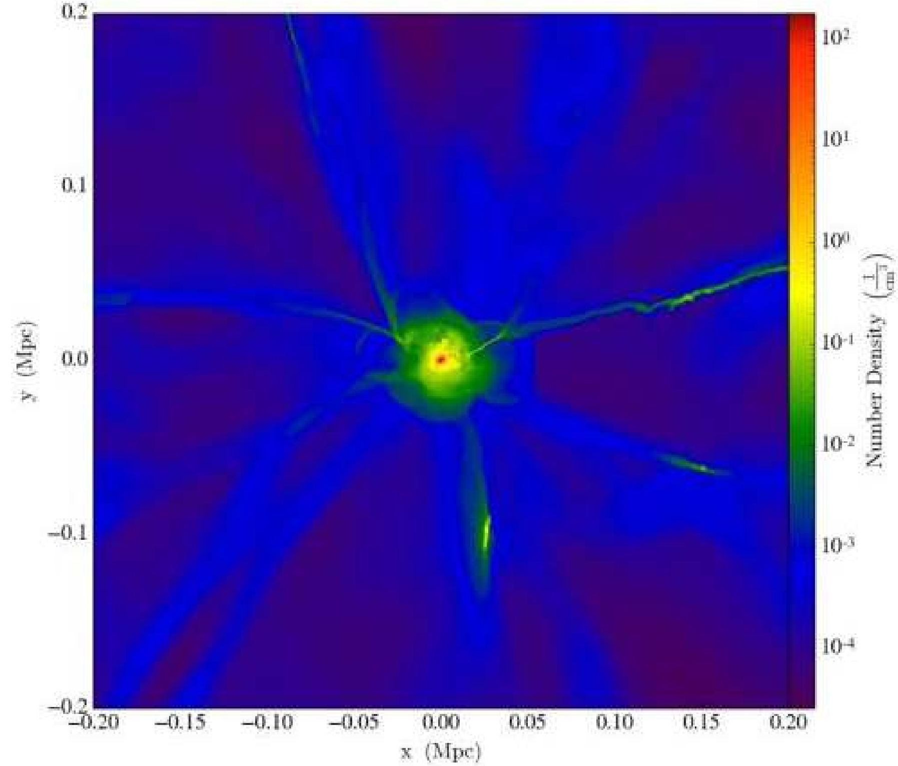


FIG. 1.— Density slice of the host halo of the quasar at $z = 7.1$. Cold accretion streams intersecting the host galaxy of the quasar are clearly visible. Distances are in comoving Mpc.

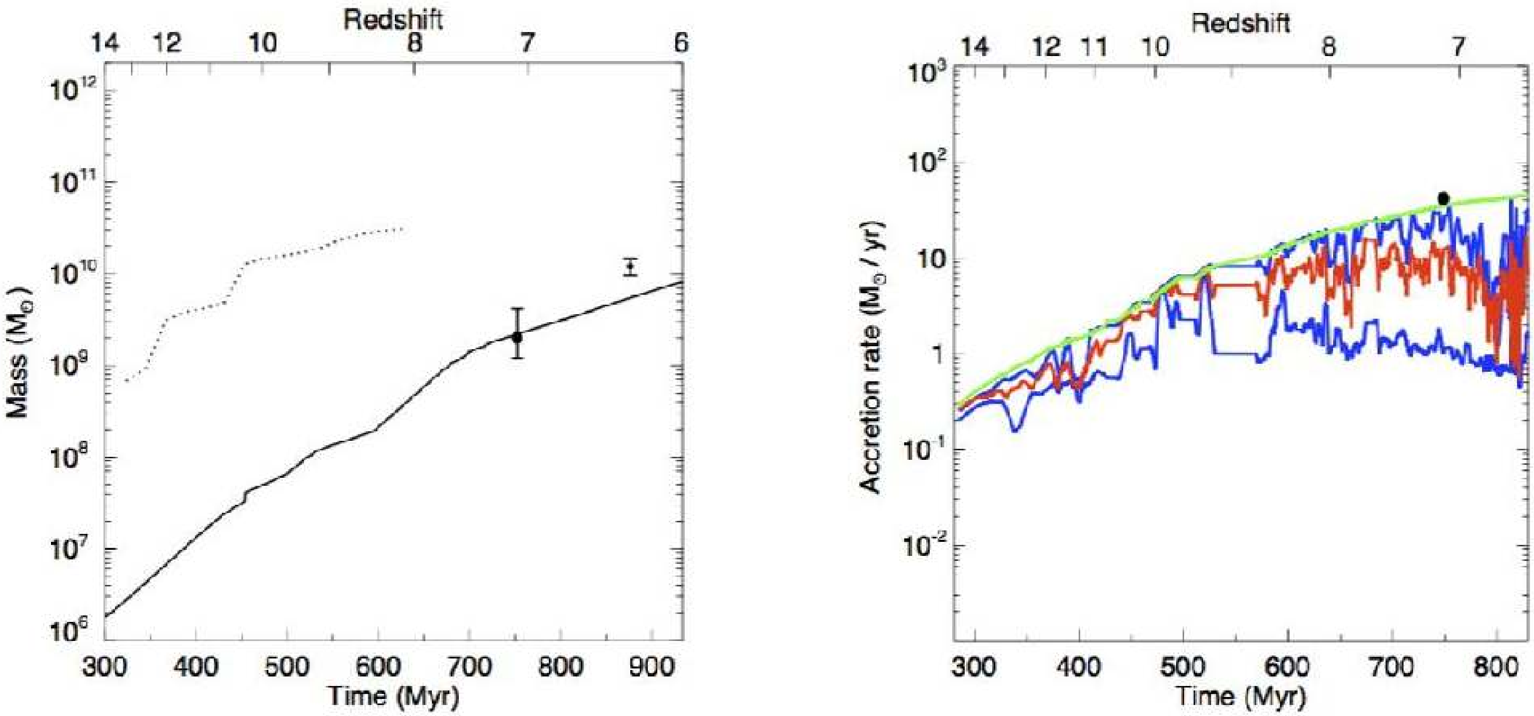


FIG. 2.— Left panel: BH mass (solid line) and halo mass (dotted line) as functions of time and redshift. The solid black circles and their error bars are the masses of J1120+0641 and J010013.02+280225.8 inferred from observations at $z = 7.1$ and 6.3, respectively. Right panel: average accretion rates (red), upper and lower limits on the accretion rate (blue) and the Eddington rate (green). The black circle is the accretion rate for the observed bolometric luminosity of J1120+0641, assuming $\epsilon = 0.1$.

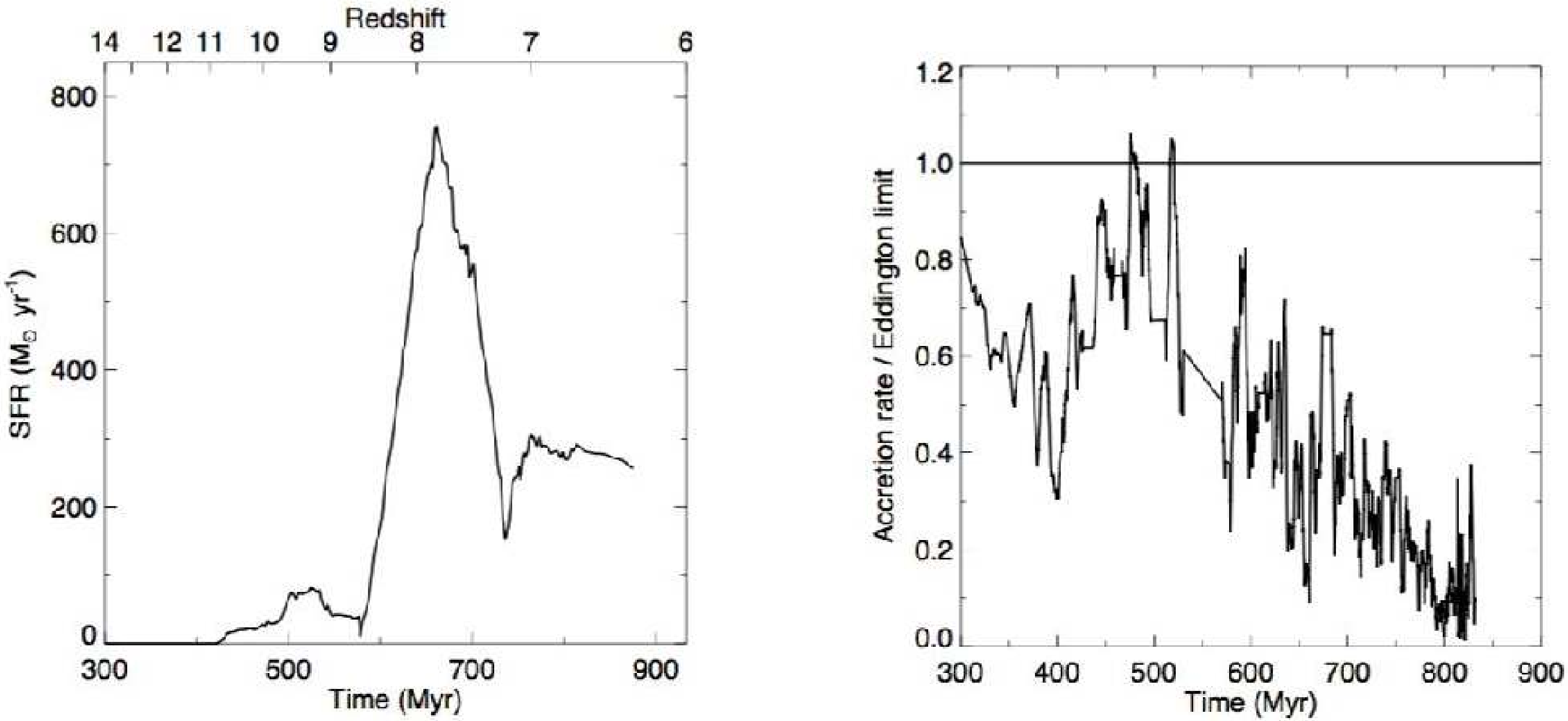


FIG. 3.— Left panel: Star formation rates in the host galaxy of the BH. Right panel: accretion rates normalized to the Eddington limit.

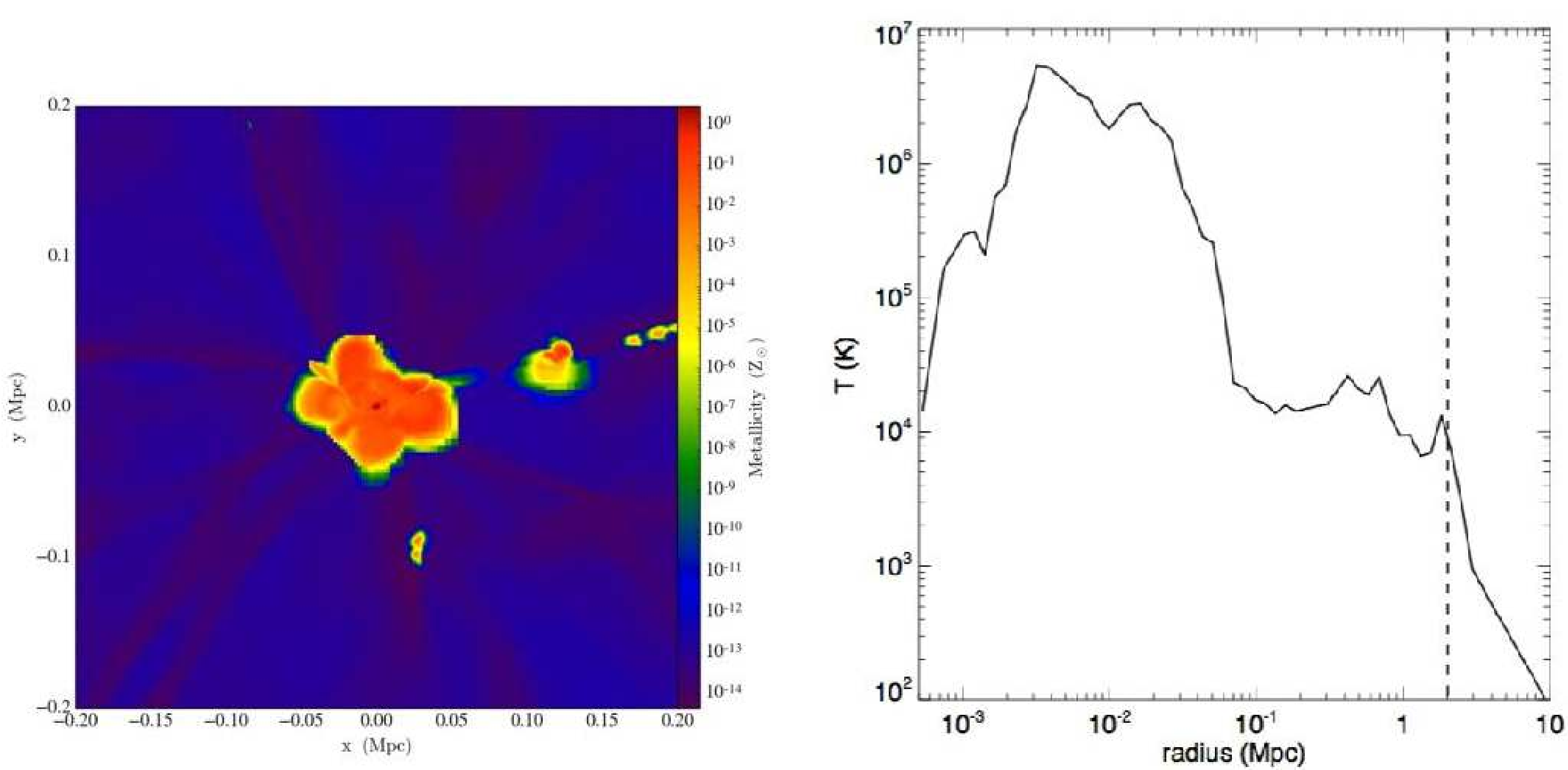


FIG. 5.— Left: metallicity slice through the center of the host galaxy of the quasar at $z = 7.1$. Distance scales are in comoving Mpc. Right: Spherically averaged temperature profile of the H II region of the quasar at $z = 7.1$. The vertical line marks the approximate boundary of gas at $> 10^4$ K at $\sim 2$ Mpc, the observed radius of the ionized near zone of ULAS J1120+0641.

# Astro-ph: 1703.00740

**Deep spectroscopy in nearby galaxy clusters: III Orbital structure of galaxies in Abell 85**

J. A. L. Aguerri[1,2★], I. Agulli[1,2,3,4†], A. Diaferio[3,4], C. Dalla Vecchia[1,2]
[1] *Instituto de Astrofísica de Canarias, C/ Vía Láctea s/n, E-38205, La Laguna, Spain*
[2] *Departamento de Astrofísica, Universidad de La Laguna, E-38206, La Laguna, Spain*
[3] *Dipartimento di Fisica, Università di Torino, Via P. Giuria 1, I-10125 Torino, Italy*
[4] *Istituto Nazionale di Fisica Nucleare (INFN), sezione di Torino, Via P. Giuria 1, I-10125 Torino, Italy*

# Черные – со спектрами, красные – члены скопления

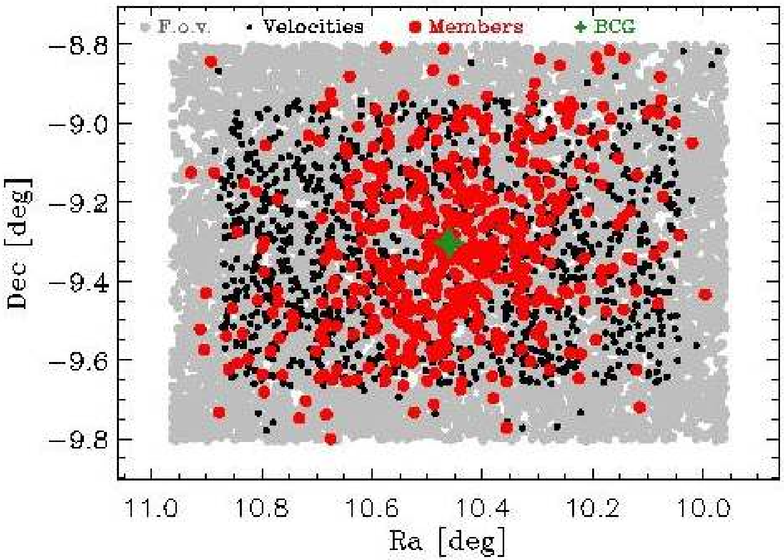


**Figure 1.** Spatial distribution of galaxies in the direction of A 85. The targets for the spectroscopic observations are shown in grey colour. They correspond to objects classified as galaxies by the SDSS-DR6 and with stellar colour $g - r = 1.0$. The black dots indicate the galaxies with measured redshift. The red dots correspond to galaxies identified as cluster members. The location of the brightest cluster galaxy is indicated by a green star.

# Главная формула

A collisionless and spherically symmetric galaxy cluster in dynamical equilibrium obeys the Jeans equation given by:

$$\frac{d}{dr}[\nu_g(r)\sigma_r^2(r)] + \frac{2\beta(r)}{r}\nu_g(r)\sigma_r^2(r) = -\nu_g(r)\frac{GM(r)}{r^2}, \qquad (1)$$

where $G$ is the gravitational constant, $M(r)$ is the total gravitational mass of the system contained in a sphere of radius $r$, $\nu_g(r)$ is the number density of cluster galaxies at radius $r$, $\sigma_r(r)$ is the radial component of the velocity dispersion, and $\beta(r) = 1 - \sigma_\theta^2(r)/\sigma_r^2(r)$ is the velocity anisotropy parameter.

# Восстановили профили плотности и дисперсии скоростей по наблюдениям

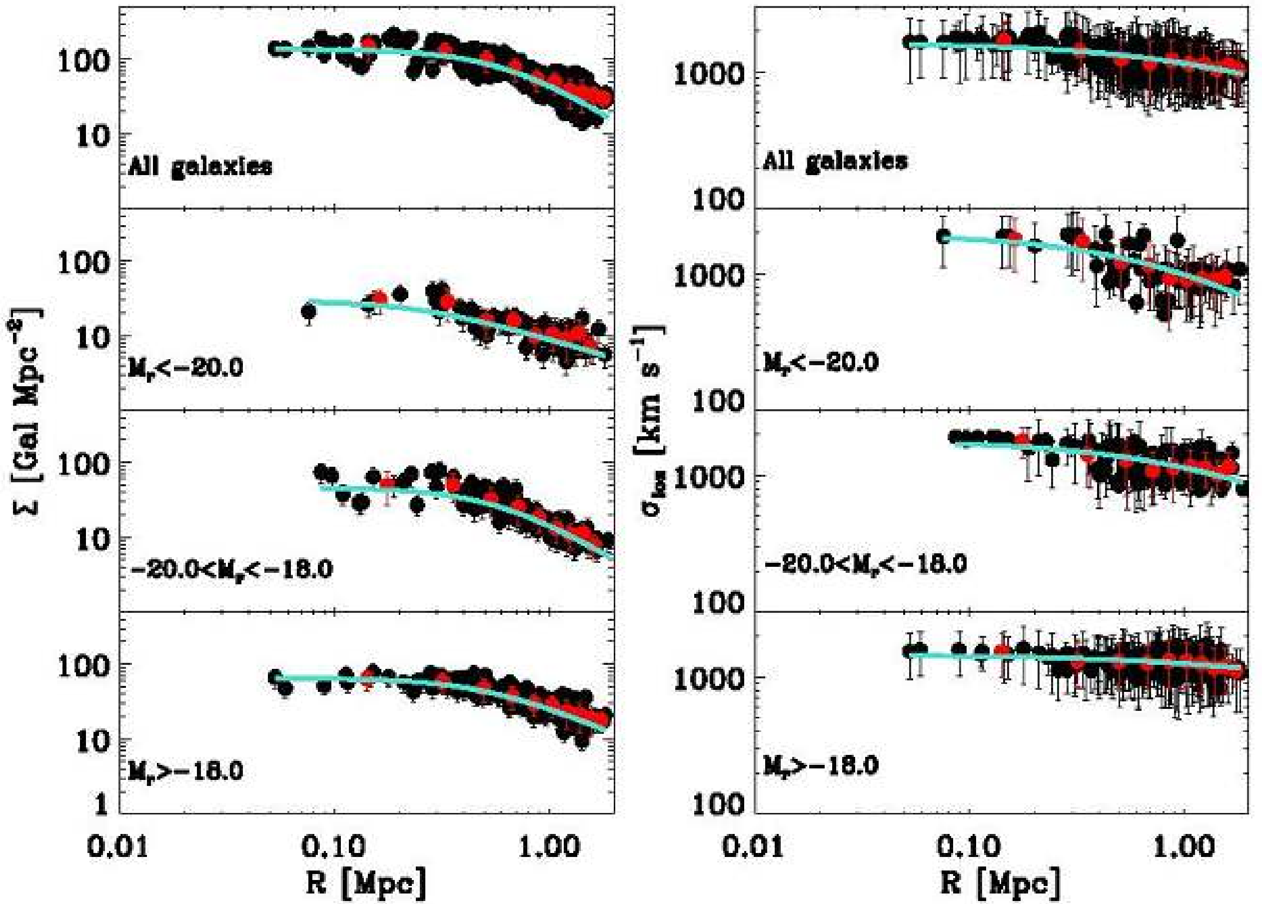


**Figure 2.** Projected galaxy number density profiles (left-hand panels) and projected velocity dispersion profiles (right-hand panels). From top to bottom we show the profiles of all the galaxies and of the galaxy sub-samples using different magnitude cuts. The black points represent the projected galaxy number density and the projected velocity dispersion at each galaxy position. The solid cyan lines are the smoothed fits of the quantities (see text for more details). The red points represent the projected galaxy number density and projected velocity dispersion obtained in radial bins.

# Голубые – те, что на круговых орбитах!

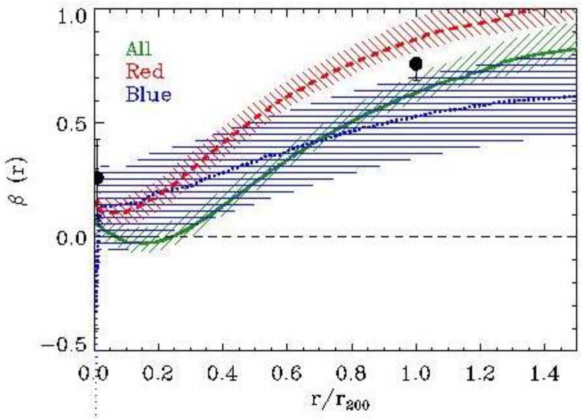


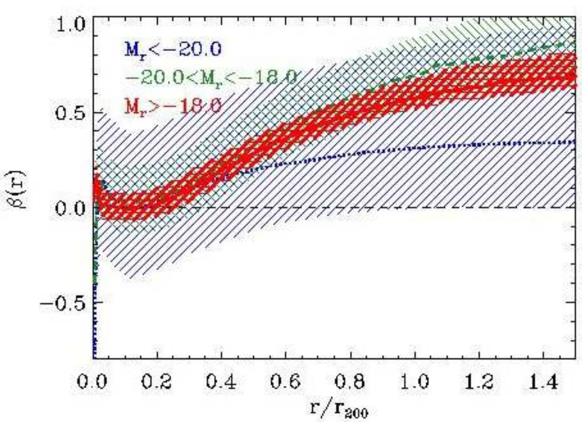


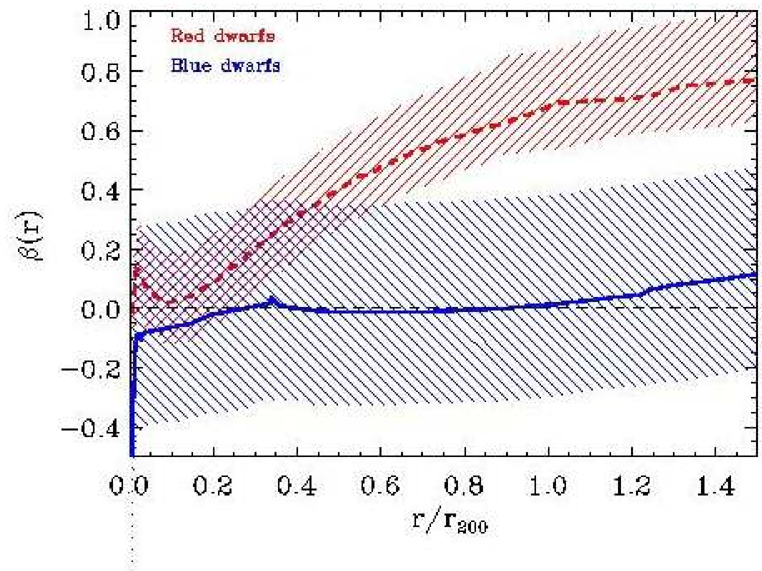


**Figure 5.** Anisotropy radial profile of blue and red dwarf galaxies of A 85. The shaded areas are similar to Fig. 3. The dash red and full blue lines correspond to red dwarf and blue dwarf galaxies, respectively

# Astro-ph: 1703.00762

## The Gaia-ESO Survey: radial distribution of abundances in the Galactic disc from open clusters and young field stars

L. Magrini[1], S. Randich[1], G. Kordopatis[2], N. Prantzos[3], D. Romano[4], A. Chieffi[5], M. Limongi[6], P. François[7], E. Pancino[1,8], E. Friel[9], A. Bragaglia[4], G. Tautvaišienė[10], L. Spina[11], J. Overbeek[9], T. Cantat-Gaudin[12], P. Donati[4], A. Vallenari[12], R. Sordo[12], F. M. Jiménez-Esteban[13,14], B. Tang[15], A. Drazdauskas[10], S. Sousa[16], S. Duffau[17,18], P. Jofré[19,20], G. Gilmore[19], S. Feltzing[21], E. Alfaro[22], T. Bensby[21], E. Flaccomio[23], S. Koposov[19], A. Lanzafame[24], R. Smiljanic[25], A. Bayo[26,27], G. Carraro[28], A. R. Casey[19], M. T. Costado[22], F. Damiani[23], E. Franciosini[1], A. Hourihane[19], C. Lardo[29], J. Lewis[19], L. Monaco[30], L. Morbidelli[1], G. Sacco[1], L. Sbordone[28], C.C. Worley[19], S. Zaggia[12]

*(Affiliations can be found after the references)*

# Выборка рассеянных скоплений

**Table 2.** Cluster parameters

| Id | R.A. | Dec. | Age | $R_{GC}$(a) | Z | rv | [Fe/H] | n. stars | Ref. Age & Distance |
|---|---|---|---|---|---|---|---|---|---|
| | J2000.0 | | (Gyr) | (kpc) | (pc) | (km $s^{-1}$) | | | |
| NGC2516 | 07:58:04 | -60:45:12 | 0.12±0.04 | 7.98±0.01 | -97±4 | +23.6±1.0 | -0.06±0.05 | 13 | Sung et al. (2002) |
| NGC6705 | 18:51:05 | -06:16:12 | 0.30±0.05 | 6.33±0.16 | -95±10 | +34.9±1.6 | +0.12±0.05 | 15 | Cantat-Gaudin et al. (2014) |
| NGC4815 | 12:57:59 | -64:57:36 | 0.57±0.07 | 6.94±0.04 | -95±6 | -29.6±0.5 | +0.00±0.04 | 3 | Friel et al. (2014) |
| NGC6633 | 18:27:15 | +06:30:30 | 0.63±0.10 | 7.71±0.01 | +52±2 | -28.8±1.5 | -0.06±0.06 | 8 | Jeffries et al. (2002) |
| NGC6802 | 19:30:35 | +20:15:42 | 1.00±0.10 | 6.96±0.07 | +36±3 | +11.9±0.9 | +0.10±0.02 | 8 | Jacobson et al. (2016) |
| Be81 | 19:01:36 | -00:31:00 | 0.86±0.10 | 5.49±0.10 | -126±7 | -126±7 | +0.22±0.07 | 13 | Magrini et al. (2015) |
| Tr23 | 16:00:50 | -53:31:23 | 0.80±0.10 | 6.25±0.15 | -18±2 | -61.3±0.9 | +0.14±0.03 | 11 | Jacobson et al. (2016) |
| NGC6005 | 15:55:48 | -57:26:12 | 1.20±0.30 | 5.97±0.34 | -141±26 | -24.1±1.34 | +0.16±0.02 | 7 | Piatti et al. (1998) |
| Pis18 | 13:36:55 | -62:05:36 | 1.20±0.40 | 6.85±0.17 | +12±2 | -27.5±0.7 | +0.10±0.01 | 3 | Piatti et al. (1998) |
| Tr20 | 12:39:32 | -60:37:36 | 1.50±0.15 | 6.86±0.01 | +136±4 | -40.2±1.3 | +0.12±0.04 | 27 | Donati et al. (2014b) |
| Be44 | 19:17:12 | +19:33:00 | 1.6±0.3 | 6.91±0.12 | +128±17 | -8.7±0.7 | +0.20±0.06 | 4 | Jacobson et al. (2016) |
| Be25 | 06:41:16 | -16:29:12 | 4.0±0.5 | 17.6±1 | -1900±200 | +136.0±0.8 | -0.25±0.05 | 6 | Carraro et al. (2005) |
| NGC2243 | 06:29:34 | -31:17:00 | 4.0±1.2 | 10.4±0.2 | -1200±100 | +60.2±0.5 | -0.38±0.04 | 16 | Bragaglia & Tosi (2006) |

# Результаты по скоплениям

**Table 3.** Clusters' elemental abundances expressed in the form 12+ log(X/H).

| Id | OI/H | MgI/H | SiI/H | CaI/H | TiI/H | ScII/H | VI/H | CrI/H | NiI/H |
|---|---|---|---|---|---|---|---|---|---|
| NGC2516 | - | 7.62±0.05 | 7.34±0.07 | 6.29±0.03 | 4.96±0.08 | 3.07±0.06 | 3.99±0.06 | 5.61±0.08 | 6.13±0.04 |
| NGC6705 | 8.75±0.06 | 7.85±0.05 | 7.59±0.04 | 6.37±0.07 | 4.93±0.07 | 3.20±0.05 | 4.05±0.10 | 5.65±0.05 | 6.34±0.03 |
| NGC4815 | 8.73±0.05 | 7.53±0.06 | 7.39±0.09 | 6.34±0.11 | 4.85±0.03 | 3.07±0.06 | 3.87±0.03 | 5.50±0.01 | 6.23±0.11 |
| NGC6633 | - | 7.58±0.03 | 7.37±0.05 | 6.31±0.05 | 4.87±0.06 | 3.05±0.04 | 3.92±0.08 | 5.61±0.06 | 6.10±0.05 |
| NGC6802 | 8.74±0.09 | 7.69±0.05 | 7.53±0.04 | 6.36±0.06 | 4.92±0.03 | 3.23±0.07 | 3.99±0.02 | 5.65±0.04 | 6.24±0.05 |
| Be81 | 8.95±0.13 | 7.87±0.06 | 7.62±0.06 | 6.52±0.05 | 5.10±0.08 | 3.39±0.05 | 4.25±0.09 | 5.84±0.07 | 6.53±0.09 |
| Tr23 | 8.84±0.07 | 7.87±0.07 | 7.66±0.05 | 6.42±0.07 | 4.96±0.07 | 3.27±0.06 | 4.09±0.06 | 5.72±0.07 | 6.35±0.06 |
| NGC6005 | 8.85±0.03 | 7.82±0.02 | 7.64±0.03 | 6.46±0.03 | 5.02±0.03 | 3.29±0.04 | 4.13±0.03 | 5.75±0.04 | 6.39±0.03 |
| Pis18 | 8.74±0.02 | 7.69±0.02 | 7.54±0.01 | 6.33±0.07 | 4.89±0.20 | 3.19±0.04 | 4.00±0.05 | 5.61±0.05 | 6.22±0.20 |
| Tr20 | - | 7.71±0.04 | 7.55±0.06 | 6.39±0.03 | 4.97±0.03 | 3.21±0.06 | 4.03±0.05 | 5.68±0.04 | 6.30±0.05 |
| Be44 | 8.84±0.20 | 7.91±0.01 | 7.73±0.02 | 6.49±0.08 | 5.13±0.03 | 3.34±0.07 | 4.24±0.04 | 5.97±0.03 | 6.45±0.03 |
| NGC2243 | 8.47±0.08 | 7.28±0.04 | 7.09±0.06 | 5.92±0.04 | 4.52±0.06 | 2.87±0.05 | 3.51±0.08 | 5.11±0.07 | 5.80±0.05 |
| Be25 | 8.90±0.18 | 7.44±0.12 | 7.26±0.08 | 6.04±0.11 | 4.69±0.08 | 3.05±0.09 | 3.70±0.07 | 5.28±0.08 | 5.96±0.08 |

# Модели (черная – современная эпоха, далее 2 и 5 млрд лет назад) в сравнении с наблюдениями рассеянных скоплений

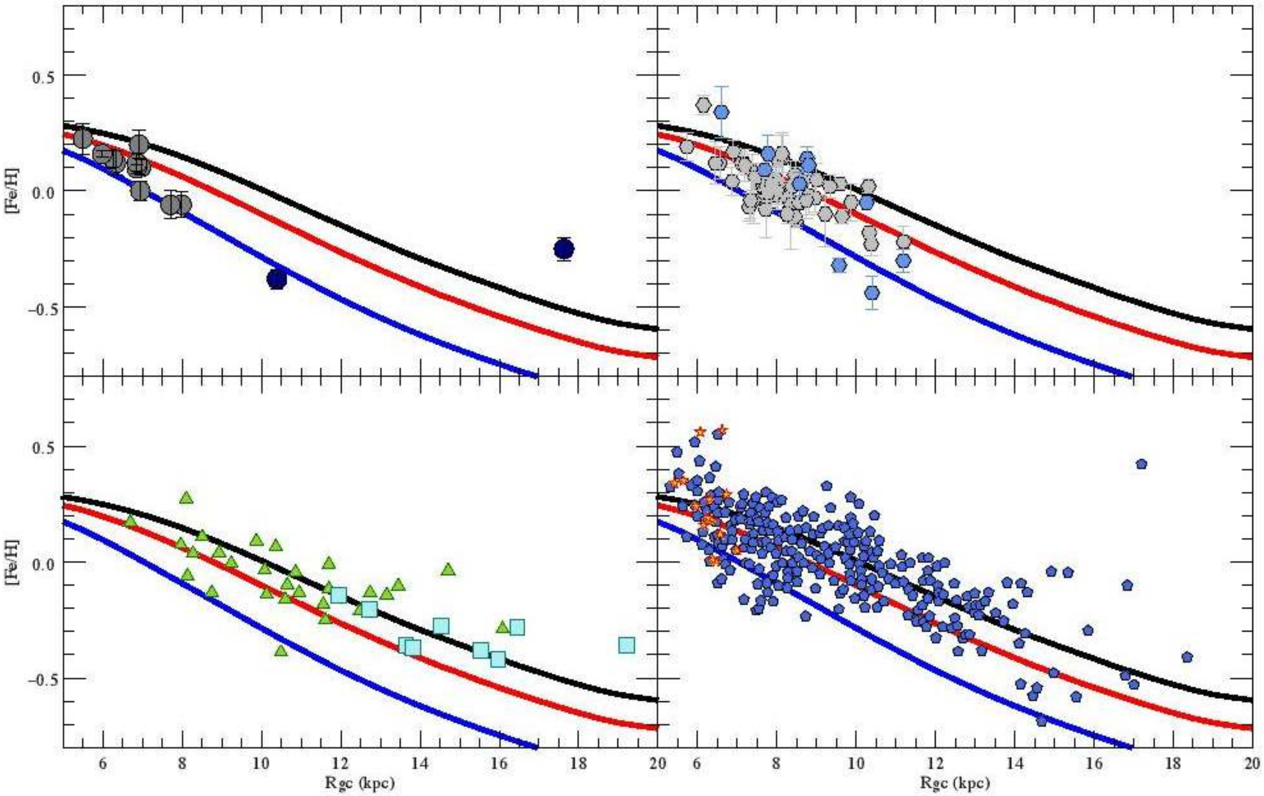

# Один из главных выводов: альфа-элементы показывают разное происхождение